Cyclic Experiments on Steel Sheet Connections for Standard CFS Framed Steel Sheet Sheathed Shear Walls

Z. Zhang, S.M.ASCE[1]; A. Singh, S.M.ASCE[2]; F. Derveni, S.M.ASCE[3]; S. Torabian, Aff.M.ASCE[4]; K. D. Peterman, M.ASCE[5]; T. C. Hutchinson, M.ASCE[6]; and B. W. Schafer, M.ASCE[7]

Abstract: The primary objective of this work is to provide connection-level force-deformation response appropriate for standard cold-formed steel (CFS) framed steel sheet sheathed shear walls under cyclic loads. Common CFS framing designs increasingly are exploring thicker framing options so that walls can meet gravity demands, overturning demands, and seismic overstrength requirements. For the seismic performance of self-drilling screw-fastened steel sheet sheathed shear walls, the cyclic nonlinear response of the screw-fastened connection is particularly important and should incorporate the impact of shear buckling of the steel sheet on the strength and ductility of the connection. Minimal cyclic connection-level shear test data exist, especially for combinations of screw-fastened thin steel sheet and thick framing steel. A unique lap shear test following current test standards was proposed to elucidate and characterize the cyclic screw-fastened connection behavior. An asymmetric cyclic loading protocol was selected with a small displacement applied in the direction that buckles the thin steel sheet, followed by progressively larger displacements in the opposite direction. A total of 93 tests were conducted, and characterization of the observed cyclic connection response with a multilinear backbone curve appropriate for use in models is provided. Connection strength is sensitive to whether the thin steel sheet ply is buckling away from or toward the fastener head in some test series. Performance of the screw shear strength as per the standard's provisions is evaluated. The work is intended to provide critical missing information for CFS framed steel sheet sheathed shear walls for use in both simulation and design. **DOI: 10.1061/(ASCE)ST.1943-541X.0003233.**

Author keywords: Earthquake engineering; Cold-formed steel (CFS); Steel sheet sheathed shear walls; Screw-fastened shear connections; Cyclic testing.

Introduction

Cold-formed steel (CFS) framed midrise structures have the potential to fulfill the need for low cost, multihazard-resilient, sustainable, and lightweight building structures. The favorable durability, ductility, high strength-to-weight ratio, stiffness, dimensional consistency, and noncombustibility of properly designed CFS framed structures afford the system potential benefits over certain aspects of competing solutions.

CFS framed steel sheet sheathed shear walls are commonly employed as one of the primary structural components providing lateral resistance in CFS framed structures (Madsen et al. 2016). A standard CFS framed steel sheet sheathed shear wall consists of single- or double-sided steel sheet sheathing, CFS studs, CFS tracks, blocking members, hold-downs or tie rods, and fasteners connecting the framing and steel sheet sheathing. Wall lines consisting of two steel sheet sheathed shear walls and an interior gravity wall were tested by Singh et al. (2021) on the shake table to investigate the wall in-plane behavior, as shown in Fig. 1(a). During the shaking, the dominant feature is the series of shear buckling waves in the steel sheet sheathing, as shown in Fig. 1(b). Peak strength and postpeak behavior is controlled largely by connection failures, as shown in Fig. 1(c). The overall shear wall response is greatly governed by the cyclic nonlinear response of the screw-fastened connection, and we also need to take the steel sheet shear buckling's effects on the connection behavior into account.

Details of the available CFS framed steel sheet sheathed shear wall tests (Singh et al. 2021; Rizk and Rogers 2017; Santos and Rogers 2017; Brière and Rogers 2017; Shamim et al. 2013; DaBreo et al. 2014; Rogers et al. 2011; Ong-Tone and Rogers 2009; Yu and Chen 2009; Yu et al. 2007; Morgan et al. 2002; Serrette et al. 1997) focused on the screw size (nominal diameters for #8, #10, and #12 screws are 4.2, 4.8, and 5.3 mm, respectively), and steel sheet and framing thickness combinations are provided in Table 1.

[1]Graduate Research Assistant, Dept. of Civil and Systems Engineering, Johns Hopkins Univ., Baltimore, MD 21218 (corresponding author). ORCID: https://orcid.org/0000-0002-4844-7907. Email: zhidongzhang@jhu.edu

[2]Graduate Research Assistant, Dept. of Structural Engineering, Univ. of California, San Diego, La Jolla, CA 92093. Email: ams082@eng.ucsd.edu

[3]Graduate Research Assistant, Dept. of Civil and Environmental Engineering, Univ. of Massachusetts, Amherst, 130 Natural Resources Rd., Amherst, MA 01003. ORCID: https://orcid.org/0000-0001-8159-0345. Email: fderveni@umass.edu

[4]Adjunct Associate Research Scientist, Dept. of Civil and Systems Engineering, Johns Hopkins Univ., Baltimore, MD 21218. Email: torabian@jhu.edu

[5]Assistant Professor, Dept. of Civil and Environmental Engineering, Univ. of Massachusetts, Amherst, 130 Natural Resources Rd., Amherst, MA 01003. Email: kdpeterman@umass.edu

[6]Professor, Dept. of Structural Engineering, Univ. of California, San Diego, La Jolla, CA 92093. ORCID: https://orcid.org/0000-0001-9109-7896. Email: tara@ucsd.edu

[7]Professor, Dept. of Civil and Systems Engineering, Johns Hopkins Univ., Baltimore, MD 21218. Email: schafer@jhu.edu

Note. This manuscript was submitted on December 24, 2020; approved on September 8, 2021; published online on November 22, 2021. Discussion period open until April 22, 2022; separate discussions must be submitted for individual papers. This paper is part of the ***Journal of Structural Engineering***, © ASCE, ISSN 0733-9445.

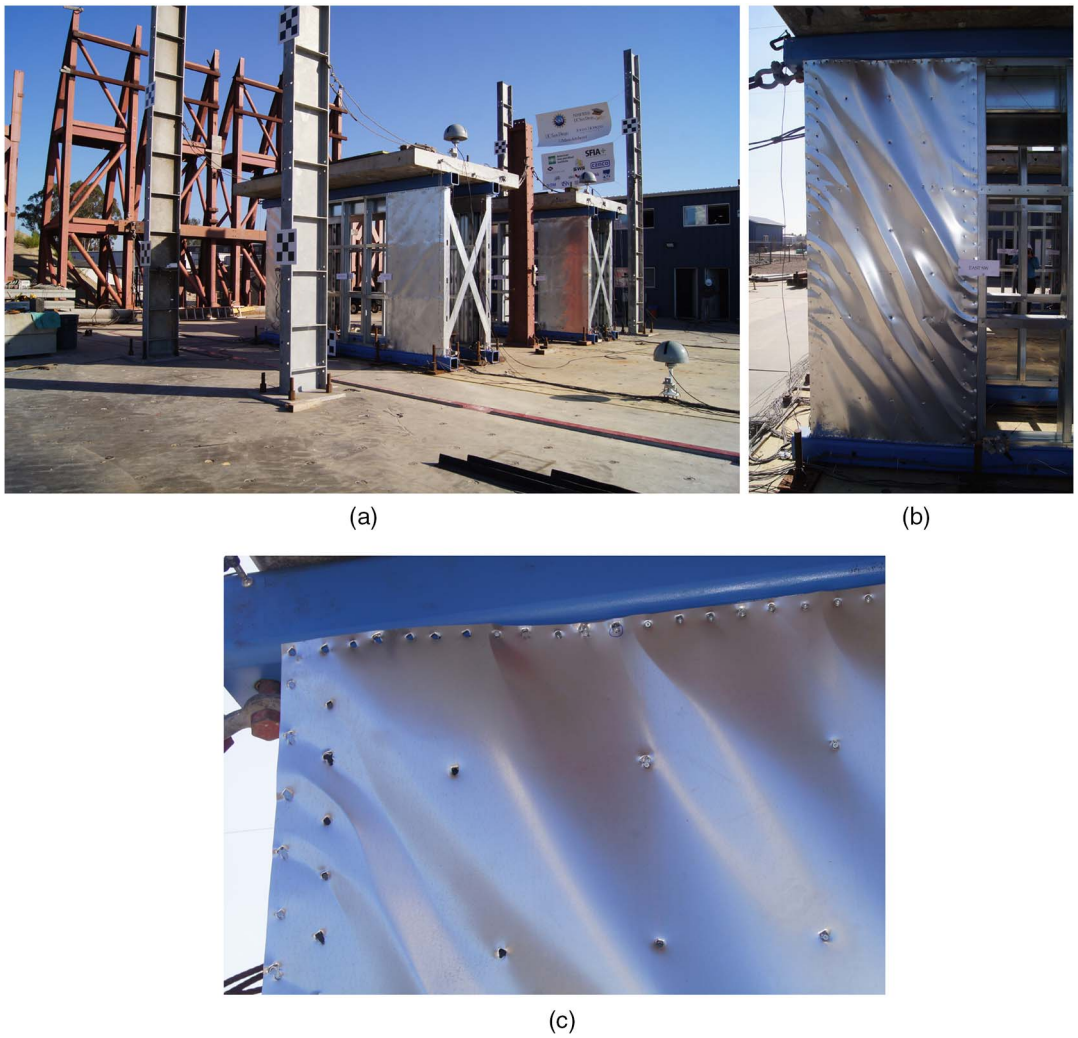

Fig. 1. CFS framed steel sheet sheathed shear wall line test of Singh et al. (2021): (a) wall line test; (b) steel sheet buckling; and (c) connection failure. (Reproduced from Singh et al. 2021.)

Table 1. Screw-fastened connections adopted in existing standard configuration CFS framed steel sheet shear wall tests

			Sheathing (mm)			Framing (mm)				
References	Load	Screw (#)	Level 1	Level 2	Level 3	Level 1	Level 2	Level 3	Level 4	Level 5
Singh et al. (2021)	Mon and Dyn	12	—	—	0.76	—	—	—	—	2.46
Rizk and Rogers (2017)	Mon and Cyc	8	—	—	0.76	—	—	1.37	1.73	2.46
Santos and Rogers (2017) and	Mon and Cyc	10	0.36	—	—	—	—	—	1.73	2.46
Brière and Rogers (2017)			0.48	—	—	—	—	—	—	2.46
		12	0.48	—	—	—	—	—	—	2.46
Shamim et al. (2013)	Dyn	8	0.46	—	—	—	1.09	1.37	—	—
			—	—	0.76	—	1.09	1.37	1.73	—
DaBreo et al. (2014)	Mon and Cyc	8	0.46	—	0.76	—	1.09	1.37	—	—
Rogers et al. (2011)	Mon and Cyc	8	0.46	—	—	0.84	1.09	—	—	—
			—	—	0.76	—	1.09	—	—	—
Ong-Tone and Rogers (2009)	Mon and Cyc	8	—	—	0.76	0.84	1.09	—	—	—
Yu and Chen (2009)	Mon and Cyc	8	0.46	0.69	—	0.84	—	—	—	—
			—	—	0.76	—	1.09	—	—	—
			—	—	0.84	—	—	1.37	—	—
		10	—	0.69	0.76	—	1.09	—	—	—
			—	—	0.84	—	1.09	1.37	—	—
Yu et al. (2007)	Mon and Cyc	8	—	0.69	—	0.84	—	—	—	—
			—	0.76	0.84	—	1.09	—	—	—
Morgan et al. (2002)	Cyc	8	—	0.69	—	0.84	—	—	—	—
Serrette et al. (1997)	Mon and Cyc	8	0.51	—	0.76	0.84	—	—	—	—

Note: Mon = monotonic tests; Cyc = reversed-cyclic (static) tests; Dyn = dynamic tests; and Level# implies steel sheathing or steel framing thickness level.

Table 2. Summary of relevant available cyclic screw-fastened connection tests

References	Screw (#)			Ply 1 (mm)	Ply 2 (mm)
Shi et al. (2018)	—	—	12	0.69	4.76
	—	—	12	1.09	4.76
Torabian and Schafer (2021)	—	10	—	0.69	0.69
	—	10	—	0.84	0.84
	—	—	12	1.09	1.09
Tao et al. (2016)	8	10	12	0.46	1.37
	8	10	12	1.09	1.37
	8	10	12	1.09	1.73
	8	10	12	1.09	2.46
Rogers and Tremblay (2003)	—	—	12	0.76	3.00
	—	—	12	0.91	3.00

With load-bearing CFS framing seeing increased use in multistory buildings, the demands on these shear walls both in terms of gravity load as well as overturning and overstrength requirements have led to the adoption of thicker framing members (e.g., increasing from 1.37 to 2.46 mm). This trend is also observed in Table 1 where the more recent testing is focusing on thicker framing members. Further, these tests demonstrate higher shear wall capacity and ductility and are thus desirable for additional reasons. Study of the cyclic performance of thin steel sheet attached to thick steel framing is needed.

Existing cyclic lap shear (or similar) connection tests (Torabian and Schafer 2021; Shi et al. 2018; Tao et al. 2016; Rogers and Tremblay 2003) are provided in Table 2, where Ply 1 is in contact with the fastener head and would be the sheet in a steel sheet sheathed shear wall and Ply 2 would be the framing. The available thickness combinations are consistent with traditional CFS construction (stud-to-track, deck-to-joist, truss diagonal to truss chord, and others) but not for steel sheet-to-framing connections. Minimal fastener-level shear test data are available for a thin steel sheet attached to thick framing.

In North America, the strength of CFS framed steel sheet sheathed shear walls is established in American Iron and Steel Institute (AISI) standard AISI S400 (AISI 2015). AISI S400-15 permits three approaches: (1) tabulated values directly from experiments; (2) an "effective strip method" (Yanagi and Yu 2014) empirically considering tension field action and limited by the connection strength; and (3) application of the principles of mechanics and supplemental data. The connection strength, typically necessary for the later two approaches and implicit in the first approach, is provided in AISI S100 (AISI 2016). Only a limited number of shear wall configurations are provided through tabulated response, and precise knowledge of the connection level behavior is necessary for determining the strength in unique cases.

The objectives of this experimental effort on steel-to-steel cyclic connection response in shear are to (1) provide results appropriate for screw-fastened steel sheet shear walls incorporating the impact of steel sheet shear buckling on the connection, (2) establish baseline behavior and characterize the connection performance, and (3) investigate the applicability of current code provisions for this connection configuration. A cyclic lap shear testing configuration following AISI S905 (AISI 2013), featuring one thin steel sheet ply and one thick framing ply connected by one single fastener with proper sensors, was designed and built. The cyclic loading protocol investigated is asymmetric, with a small displacement applied in the direction that buckles the thin steel sheet, followed by progressively larger displacements in the opposite direction.

The test data are idealized with a multisegment linear backbone phenomenological model to support the design and high-fidelity finite element model development for CFS framed steel sheet sheathed shear walls. This paper provides the technical details and processing of 93 conducted tests on steel sheet connections for CFS framed screw-fastened steel sheet sheathed shear wall configurations covering a wide range of framing thickness, sheet thickness, fastener size, and loading type.

Screw-Fastened Connection Failure Modes

In addition to strength, the manner in which these connections fail is also of interest. Because the dominant deformation in the screw-fastened connection is shear, the primary mode of behavior is bearing in the steel sheet, and for some thickness ranges, tilting. However, disengagement of the stud and sheet is the ultimate failure mode, and four modes are also commonly observed, three primarily associated with tensile demands on the connection, namely pull-through, pull-through with tilting and bearing, and pull-out, and one associated with shear, namely shear rupture (or edge tear out), as illustrated in Fig. 2.

Pull-through, as shown in Fig. 2(a), is not specifically defined in AISI S100 (AISI 2016), but is recognized in the related technical literature (Peterman et al. 2014) and is close in behavior to pull-over. In the shear wall, pull-through develops when the stud or track flange deforms and pulls the fastener with it, resulting in the fastener head tearing through the sheet. If the stud or track deformation involves much twisting, then the failure mode is pull-through with tilting and bearing as shown in Fig. 2(b). Finally, if instead of the sheet tearing, the threads pull-out of the stud or track, then pull-out, as shown in Fig. 2(c), is the observed failure mode. For shear rupture, the most common failures occur due to minimal edge distance limiting the bearing capacity, as shown in Fig. 2(d). Per AISI S100 (AISI 2016), screw shear must also be considered; however, due to the presence of the thin steel sheet, screw shear does not occur in any of the connections considered herein.

Experimental Program

Test Matrix

The fastener and sheet ply thicknesses selected in this testing program are summarized in Table 3. The test specimen consists of one thick steel framing ply and one thin steel sheet ply (in contact with the screw head) fastened by a single screw. This test matrix is designed considering both the existing screw-fastened connection and shear wall test data and covering a wide range of steel sheet thickness, fastener size, and various loading types. Only one relevant configuration has both connection and steel sheet shear wall data; otherwise there is a poor match between available connection data and tested shear walls, and a distinct need to test configurations with thicker framing steel.

As listed in Table 3, in a standard test series, there are seven tests, including one monotonic test, three asymmetric cyclic tests with thin sheet buckling away from the fastener head, and three asymmetric cyclic tests with thin sheet buckling toward the fastener head. The necessity to force the thin sheet buckling direction was demonstrated in shakedown tests (Zhang and Schafer 2020) and is discussed further in the results. Each test series is given a nomenclature, e.g., the 54-8-30 series stands for a thick 1.37-mm (54-mil) framing steel ply fastened with a single #8 self-drilling screw to a thin 0.76-mm (30-mil) steel sheet ply. As indicated in Table 3, in the 97-10-30 series, three additional tension-only cyclic tests are

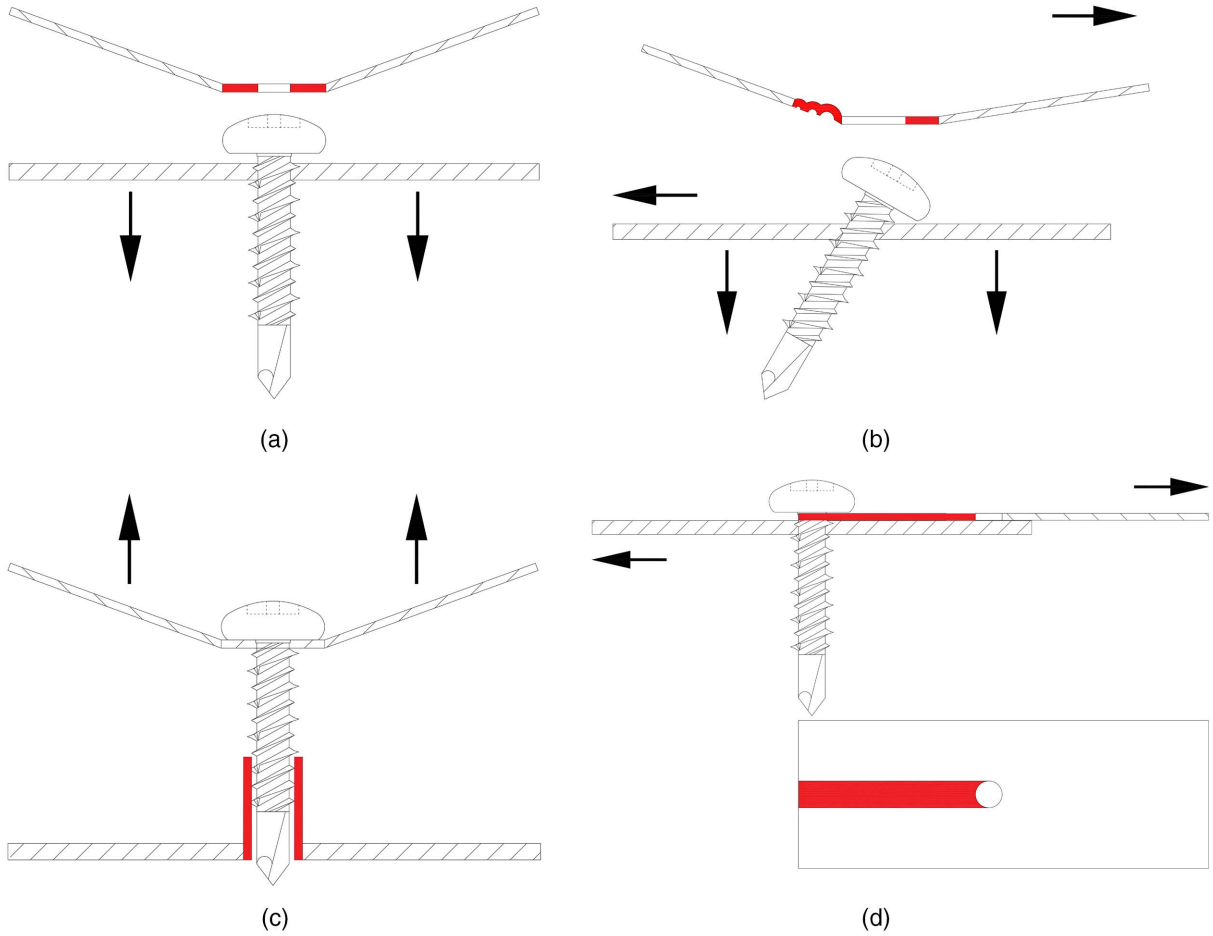

Fig. 2. Screw-fastened connection failure mechanism: (a) pull-through; (b) pull-through with tilting and bearing; (c) pull-out; and (d) shear rupture.

completed, for a total of 10 tests. To verify results, additional repetitions were conducted in some cases, resulting in a total of 93 tests completed versus 80 tests originally proposed in the test matrix. Each test conducted is assigned a unique test number, and all individual results are available in a comprehensive test report (Zhang and Schafer 2020).

Test Specimens

The standard lap-joint shear test specimen configuration per AISI S905 (AISI 2013) is not able to capture the steel sheet buckling behavior and resulting pull-through screw-fastened connection failure mode; therefore, the test specimen needs to be specially designed based on the failure modes observed in shear wall tests as shown in Fig. 2 and previously detailed. Due to the shear buckling of the steel sheet, the perimeter fasteners not only resist shear demand but also must resist out-of-plane forces that work on the fastener head. The force caused by the sheet buckling itself is not a large demand, but can lead to premature pull-through behavior as opposed to pure bearing in a connection. This shear–tension interaction of interest in this testing program is identical with the connection behavior and overall shear wall response under seismic events.

Simple modifications to the dimensions and loading protocol of a standard lap shear joint test are adopted to provide these additional conditions. As shown in Fig. 3, the upper and bottom shaded parts with 50.8-mm (2-in.) length are clamping areas for the grips, and 50.8-mm (2-in.) × 50.8-mm (2-in.) spacers are placed inside the grips to avoid eccentric loading. The thin steel sheet ply length is set equal to the half-wave length of steel sheet sheathing close to the shear wall framing boundary. After reviewing typical shear wall tests including W2 test by Rizk and Rogers (2017), W21 test by Santos and Rogers (2017), and M11 test by Yu et al. (2007), a simple estimate for the shear buckling half-wave length in the perimeter is approximately 102-mm (4-in.). This distance then corresponds to the length between the top grip and fastener head of the specimen.

The edge distance for the thick framing ply is chosen to be 20.6-mm (0.81-in.), which corresponds to half of the flange width

Table 3. Test matrix and existing related data for steel framing-to-steel sheet screw-fastened connection tests

Framing steel [mm (mil)]	Steel sheet [mm (mil)]								
	0.33 (13)			0.48 (19)			0.76 (30)		
	#8	#10	#12	#8	#10	#12	#8	#10	#12
1.37 (54)	7	7	—	7[a]	7[b]	[b]	7[c]	7[c]	—
2.46 (97)	—	7[c]	—	—	7[c]	[c]	7[c]	10	7[c]

[a]Range of existing screw-fastened connection tests matching shear wall tests.
[b]Range of existing screw-fastened connection tests.
[c]Range of screw-fastened connections adopted in the existing steel sheet shear wall tests.

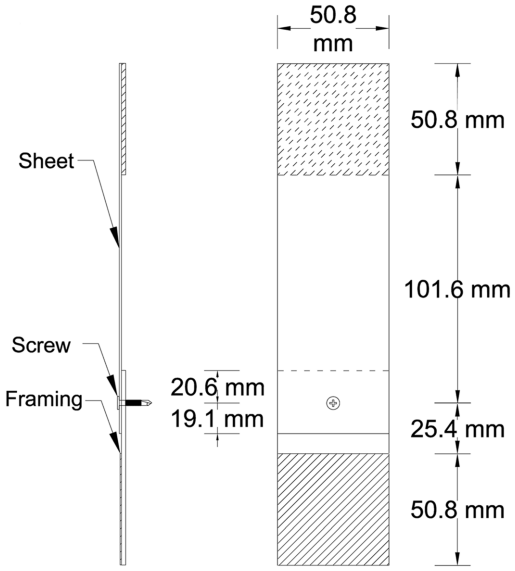

Fig. 3. Test specimen.

of a typical chord stud section (362S162-97). The edge distance for the thin steel sheet ply is set at 19.1-mm (0.75-in.), which meets the 1.5d minimum edge distance requirement in J4.2 of AISI S100 (AISI 2016), where d is the nominal screw diameter. The length between the fastener and bottom grip is minimized to 25.4-mm (1-in.) to minimize tilting of the steel ply in a standard lap-joint shear test per AISI S905 (AISI 2013). All the specimens were assembled in the Thin-walled Structures Laboratory at Johns Hopkins University using a HILTI ST 1800 screw gun (Plano, Texas) with a torque setting between 8 and 12 N · m. A pilot hole was employed for the thick 2.46-mm (97-mil) framing ply with #8 screws; otherwise the self-drilling screws were used directly without a pilot hole.

Test Setup

A test rig as presented in Fig. 4(a) was designed and constructed. All the tests were conducted in an MTS servohydraulic test system (Eden Prairie, Minnesota). A position transducer (PT) and a load cell are adopted to acquire deformation and force data. In addition, a laser displacement sensor is utilized to monitor the out-of-plane thin steel sheet buckling deformation. A mechanical lateral support is installed at either left or right side to guide the thin sheet to buckle away or toward the fastener head. A typical test specimen in the test rig is presented in Fig. 4(b). Figs. 4(c and d) show the typical specimen's response in tension and compression.

For the specimen under tension, the force-displacement curve provides the bearing stiffness and connection strength in shear, and when the specimen is in compression the force-displacement curve simply reflects the thin steel sheet buckling strength. One-sided cyclic lap shear testing is adequate for capturing the shear behavior because previous cyclic testing demonstrated that the response is symmetric (Torabian and Schafer 2021; Shi et al. 2018; Tao et al. 2016). Further, the buckling of the thin steel sheet creates a shear–tension interaction on the connection consistent with screw-fastened connections in steel sheet shear walls, and maximizes the

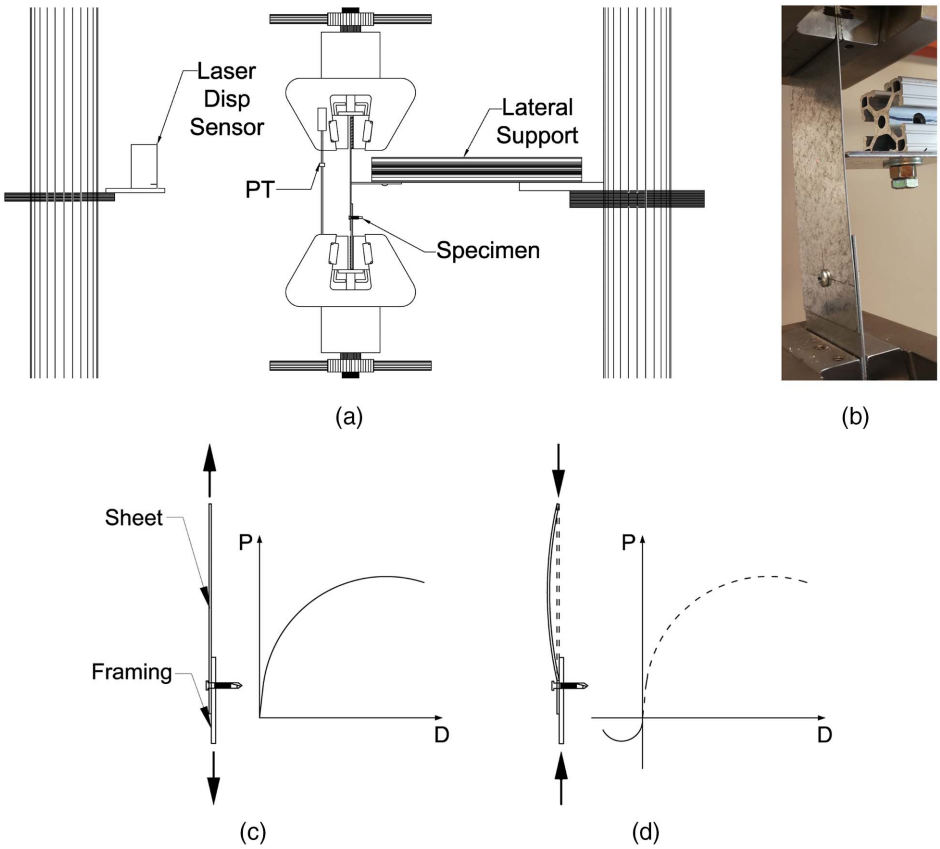

Fig. 4. Test rig and specimen: (a) test setup; (b) test specimen in the testing rig; (c) test specimen response in tension; and (d) test specimen response in compression.

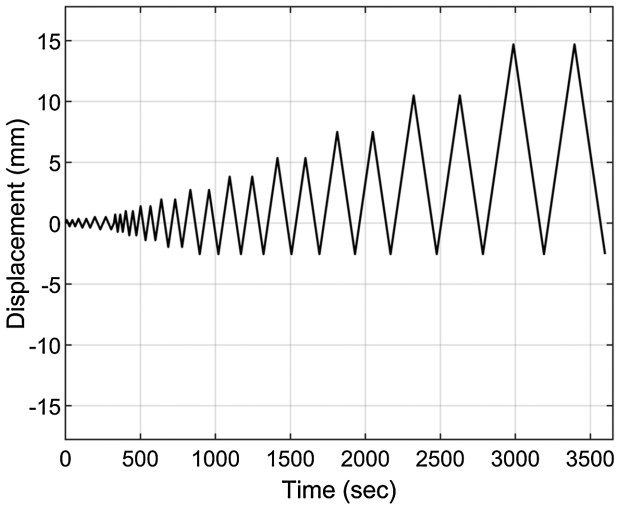

Fig. 5. Asymmetric cyclic loading protocol.

opportunity that the fastener tilts and slips through the thin steel sheet.

Loading Protocol

Consistent with other recently completed CFS connection-level cyclic shear tests (Torabian and Schafer 2021; Shi et al. 2018; Tao et al. 2016), we implemented the FEMA 461 quasi-static loading protocol (FEMA 2007) in this test program. The loading protocol is modified to incorporate a small magnitude of compression displacement: 2.5-mm (0.1-in.), which is estimated using a sine wave approximation for the buckling wave (Zhang and Schafer 2020) with out-of-plane buckling deformation equal to 10.2-mm (0.4-in.) based on the shell finite-element simulation of steel sheet shear walls in ABAQUS version 6.13 (Zhang and Schafer 2019).

As illustrated in Fig. 5, the modified FEMA 461 loading protocol demonstrates two repeated symmetric cycles increasing in magnitude by a factor of 1.4 until the compression displacement exceeds 2.5-mm (0.1-in.) and subsequent two repeated asymmetric cycles with only tension side increase by a factor of 1.4. The loading rate is 0.028 mm/s (0.0011 in./s) in the initial six cycles, and later cycles employ a 0.084 mm/s (0.0033 in./s) loading rate. For the conducted monotonic tests, the tests follow the AISI S905 (AISI 2013) using a loading rate of 0.021 mm/s (0.00083 in./s).

Test Results

Material Testing

Three standard tensile coupons per ASTM E8/E8M (ASTM 2016) for each thickness of sheet material were tested. The coupons were tested with coating, then the zinc coating at the two ends of the coupon was stripped with hydrochloride acid (HCL-1N) to accurately measure the base metal thickness. The specimens were loaded at a rate of 0.021 mm/s (0.00083 in./s). The test results including yielding stress $f_{0.2}$ (0.2% offset method), strain at yielding ε_y, tensile strength f_u, strain at tensile strength ε_u, and the total elongation ratio ε_r are provided in Table 4. The thin sheet materials tend to demonstrate lower yield stress and higher elongation, which aligns with the CFS framed steel sheet sheathed shear wall design philosophy that the steel sheet sheathing works as an energy-dissipating fuse with lower yield stress and higher ductility.

Table 4. Material test results

Nominal thickness [mm (mil)]	Measured thickness (mm)	f_{yn} (MPa)	$f_{0.2}$ (MPa)	f_u (MPa)	ε_u (%)[a]	ε_r (%)[b]
0.33 (13)	0.31	345	332.42	415.84	17.64	26.36
0.48 (19)	0.48	227	208.99	343.72	21.79	40.95
0.76 (30)	0.78	227	150.37	312.11	22.32	46.04
1.37 (54)	1.47	345	354.63	466.24	20.15	36.57
2.46 (97)	2.54	345	422.43	534.21	10.75	16.18

[a]Strain at tensile strength ε_u is achieved using an extensometer with 25.4-mm gauge length and 5.1-mm maximum range.
[b]Total elongation ratio ε_r is based on the measured distance between two manually drawn lines before testing with 51-mm gauge length.

Results Summary

Table 5 provides key summary statistics for the conducted tests under cyclic loading, averaged by test series. Stiffness and strength are largely governed by sheet thickness, with fastener size and framing thickness playing secondary roles. The initial stiffness k_0 is estimated based on the response at 40% of the peak strength (P_{peak}). Deformation corresponding to the peak strength is denoted as D_{peak}, and deformation corresponding to the 80% postpeak force level is denoted as $D_{80\%}$.

Typical Behavior and Failure Modes

Dominant failure modes observed in the testing are (1) bearing, (2) tilting and bearing, (3) pull-through with tilting/bearing, and (4) shear rupture. Bearing, or bearing and tilting, is always developed prior to disengagement by either pull-through or shear rupture. The pull-through with tilting/bearing failure mode, as depicted in Fig. 2(b), occurs only after bearing or tilting and bearing failure modes have been initiated and is accompanied by tearing of the thin steel sheet ply area in contact with the fastener head, and is subsequently described as pull-through herein. A plastic hinge always forms in the middle of the thin steel sheet after a small number of compression cycles. In each test, deformation and development of the failure modes are carefully observed. Images were selected as close as possible to the specific force levels.

The most important consideration in describing the observed behavior in the tests is the difference in thickness between the thick (framing) ply and the thin (sheet) ply. For connection configurations with the framing and sheet thickness far apart, such as the 54-8-13 test series, bearing dominates (Zhang and Schafer 2020); a representative test is shown in Fig. 6.

For the case where the thin steel sheet ply is constrained to buckle toward the fastener head, the pull-through failure mode is incorporated into the bearing behavior after the peak force level, and is ultimately accompanied by the edge tear out and disengagement of the fastener from the thin steel sheet ply. In the tension cycles, bending of the thin steel sheet ply edge is initialized by the fastener prying and develops as the test progresses. There is no obvious deformation in the 1.37-mm (54-mil) framing ply. In general, little difference is observed between forcing the thin ply buckling away from or toward the fastener head. Similar overall observations can be found in most tests with a 0.33-mm (13-mil) or 0.48-mm (19-mil) steel sheet ply.

When the framing and sheet are relatively close in thickness, including the 54-8-30 and 54-10-30 test series, the results are observed to be sensitive to whether the thin steel sheet ply is buckling away from or toward the fastener head. In the 54-8-30 test series, where the thin steel sheet ply is constrained to buckle away from

Table 5. Average test results for cyclic tests

Test series	Screw (#)	Sheet [mm (mil)]	Framing [mm (mil)]	No. of tests	k_0 (kN/mm)	D_{peak} (mm)	P_{peak} (kN)	$D_{80\%}$ (mm)
54-8-13	8	0.33 (13)	1.37 (54)	7	8.11	1.04	1.14	3.73
54-10-13	10	0.33 (13)	1.37 (54)	7	6.55	1.07	1.34	3.87
97-10-13	10	0.33 (13)	2.46 (97)	7	14.68	0.10	1.51	2.77
54-8-19	8	0.48 (19)	1.37 (54)	7	9.75	3.39	1.67	5.19
54-10-19	10	0.48 (19)	1.37 (54)	7	10.13	3.36	1.88	5.18
97-10-19	10	0.48 (19)	2.46 (97)	7	12.80	2.88	1.75	5.49
54-8-30	8	0.76 (30)	1.37 (54)	8	5.33	12.55	4.14	14.13
54-10-30	10	0.76 (30)	1.37 (54)	11	11.65	10.23	4.08	12.14
97-8-30	8	0.76 (30)	2.46 (97)	9	21.75	5.32	3.56	7.18
97-10-30	10	0.76 (30)	2.46 (97)	14	16.80	5.70	3.41	7.52
97-12-30	12	0.76 (30)	2.46 (97)	9	27.51	5.45	3.51	7.36

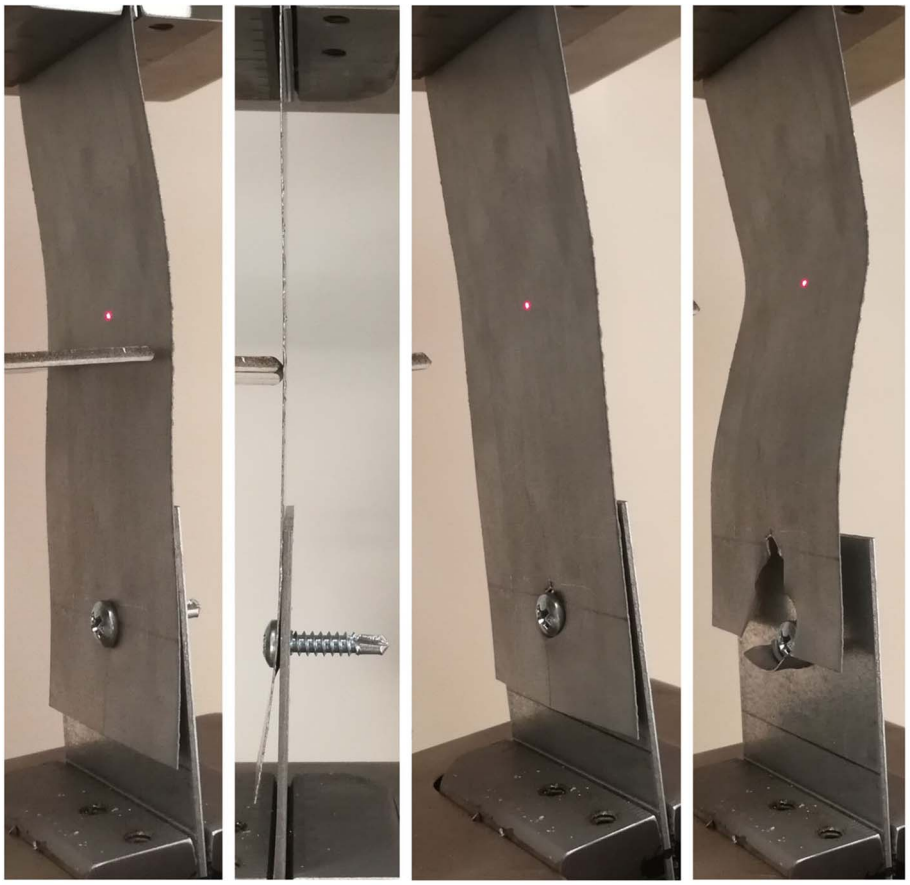

Fig. 6. Deformation and failure of a test in the 54-8-13 test series: (a) peak strength level front view; (b) peak strength level side view; (c) 80% postpeak strength level; and (d) after test.

the fastener head, primarily pull-through, with tilting and bearing, is the observed failure mode (Zhang and Schafer 2020), as shown in Fig. 7. Pull-through ultimately triggers disengagement of the fastener from the thin steel sheet ply [it is not obvious in Fig. 7(d), but when the specimen is in compression, the disengagement is readily observed].

The demand on the fastener in the test is primarily shear, with a small amount of tension in the prepeak load regime and shear–tension interaction (demand) at and after the peak load. Bending of the thin 0.76-mm (30-mil) steel sheet ply edge is initialized by fastener prying and continues throughout the test. Also, past the peak load, the pull-through limit state is accompanied by the fastener head tearing the thin steel sheet ply area in contact with the fastener head. Minor bending deformation of the thicker 1.37-mm (54-mil) framing steel ply is identified, but remains relatively small throughout the test.

In the 54-8-30 test series where the thin steel sheet ply is constrained to buckle toward the fastener head bearing, fastener tilting and shear rupture are observed (Zhang and Schafer 2020), as shown in Fig. 8. Bearing, fastener tilting, and shear rupture limit states are all observed in the thinner 0.76-mm (30-mil) sheet ply throughout the test, and demand for the fastener is predominately shear.

Fig. 7. Deformation and failure of a 54-8-30 test with thin sheet buckling away from the fastener head: (a) peak strength level front view; (b) peak strength level side view; (c) 80% postpeak strength level; and (d) after test.

The tearing deformation (shear rupture) of the thin steel sheet ply demonstrating longitudinal shearing of the thin steel sheet along two approximately parallel planes is initialized prior to peak load and develops as the test progresses until disengagement. Minor bending in the thick 1.37-mm (54-mil) framing is observed throughout the test.

Sensitivity in strength and observed failure mode to the buckling direction of the thin steel sheet ply is not universal. In some connection configurations with framing-to-sheet thickness ratio between the aforementioned two cases, including 97-8-30, 97-10-30, and 97-12-30 test series, the buckling direction (away or toward) influences the observed behavior in only one or a few cases in the same test series. No fastener tilting is observed in the tests with these configurations because the 2.46-mm (97-mil) framing steel is quite stiff. Bearing and pull-through are the dominant failure modes for most asymmetric cyclic tests with these connection configurations.

A representative test in the 97-12-30 test series, with the thin steel sheet constrained to buckle away from the fastener head (Zhang and Schafer 2020), is shown in Fig. 9. The bearing limit state is observed in the thinner sheet ply throughout the test, and the pull-through limit state gradually develops after peak load. Another test in the same 97-12-30 test series with the thin steel sheet constrained to buckle toward the fastener head (Zhang and Schafer 2020) is depicted in Fig. 10. Different from the former test, bearing and shear rupture are the dominant failure modes for this test, and the demand on the fastener is predominately shear.

Force-Displacement Response

The observed force-displacement response is highly nonlinear, but overall trends based on the relative difference in thickness between the two steel plies are still readily observed. Response in the test series when the thickness of the framing ply and sheet ply are relatively similar are provided in Fig. 11, and when the thickness of the two plies are far apart in Fig. 12.

The 54-8-30 test series responses as provided in Fig. 11(a) are representative of configurations with similar framing thickness and steel sheet thickness. Fig. 11(a) indicates if the response is sensitive to whether the thin steel sheet ply (in contact with the fastener head) is buckling away from (denoted with an A) or toward the fastener head (denoted with a T) in the compression cycles. The monotonic test is denoted with the letter M, and the first number within the test nomenclature in the legend represents the unique test ID.

The buckling-away cases create additional tension demand on the connection, which triggers the pull-through limit state and

Fig. 8. Deformation and failure of a 54-8-30 test with thin sheet buckling toward the fastener head: (a) peak strength level front view; (b) peak strength level side view; (c) 80% postpeak strength level; and (d) after test.

degrades the strength and postpeak shear behavior. In the buckling-toward cases, the thin steel sheet ply tends to flatly align with the shear load path, and the fastener head does not create additional tension demand on the connection, resulting in only bearing and no pull-through limit state. The dominant limit states are bearing and shear rupture, which results in higher strength. Moreover, buckling-toward cases demonstrating higher test strength than the buckling-away cases can also be observed in other configurations, including the 54-10-30, 97-8-30, and 97-12-30 test series, as shown in Figs. 11(b–d).

When the framing thickness and steel sheet thickness are far apart, the test strength is not sensitive to whether the thin steel sheet ply is buckling away from or toward the fastener head, as shown in Fig. 12. For example, as provided for the 54-8-13 test series in Fig. 12(a), strength and postpeak behavior are consistent across tests, regardless of load type and buckling direction. The thin 0.33-mm (13-mil) steel sheet ply is thin and flexible under compression demand and does not significantly influence the connection behavior. The prepeak load response is dominated by bearing, but the combined shear–tension interaction demand on the connection triggers the pull-through limit state and ultimately disengagement of the parts. The same insensitivity to whether the thin steel sheet ply is buckling away or toward the fastener head can also be observed in the 54-10-13, 54-8-19, 54-10-19, 97-10-13, and 97-10-19 test series, as shown in Figs. 12(b–f), respectively.

For the 97-10-30 test series, as provided in Fig. 13, three additional tension-only cyclic tests with thin steel sheet buckling away the fastener head were conducted to examine the impact of the loading protocol on the response. As presented in Fig. 13, the tension-only cyclic tests (denoted by Ten) have higher strength than the monotonic and buckling-away cases [average of 3.31 kN (0.744 kip) for the Ten tests, 3.21 kN (0.722 kip) for the M test, and 3.25 kN (0.731 kip) for the A tests], but the postpeak shear behavior, and limit states are the same. This implies that the small compression cycles do create meaningful degradation in strength. Therefore, asymmetric cyclic lap shear testing with a small compression displacement is adequate, and potentially necessary, to study the impact of cyclic sheet buckling on the performance of connections in steel sheet shear walls.

The relationship between force and lateral displacement of the centerline at the thin steel sheet was also recorded in the testing. The compression displacement of 2.5-mm (0.1-in.) typically resulted in lateral deformation at center of the thin sheet up to 10.2-mm (0.4-in.) in elastic range and up to 30.5-mm (1.2-in.) when the plastic hinge developed. Complete details are provided in the test report (Zhang and Schafer 2020).

Fig. 9. Deformation and failure of a 97-12-30 test with thin sheet buckling away from the fastener head: (a) peak strength level front view; (b) peak strength level side view; (c) 80% postpeak strength level; and (d) after test.

Connection Behavior Characterization

Multisegment Linear Backbone Curve

To provide a convenient means to implement the tested connections in models a procedure is developed for idealizing the test results with a multisegment linear backbone phenomenological model. A four-segment model, consistent with the Pinching4 material model in OpenSees version 3.2.2 (Mazzoni et al. 2006), is selected for the backbone. The model is fit by balancing energy between the linear segment model and the nonlinear test result. Only the tension side test result is adopted for the data characterization herein. As illustrated in Fig. 14(a), the developed modeling parameters (D_1, P_1; D_2, P_2; D_3, P_3; and D_4, P_4) are intended to support numerical models that need to simulate the nonlinear (hysteretic) screw-fastened connection response, e.g., in a shear wall simulation. Test data characterization detailed results are tabularized and provided in the test report (Zhang and Schafer 2020).

An asymmetric cyclic test in the 54-8-30 test series (Zhang and Schafer 2020) is adopted herein to detail the characterization procedure. As shown in Fig. 14(b), the procedure first generates an idealized backbone based on the test data, composed of the peak load point of each loading step before the last loading cycle and the peak displacement point of the last loading cycle. Then, a multisegment linear backbone model is developed based on energy dissipation balance (i.e., the accumulative product of force and displacement) between the idealized backbone and the multisegment linear backbone model. The multisegment linear backbone model consists of four points, as shown in Fig. 14(a), where the third point is the peak strength point in the test curve, and the strength values of the first, second, and fourth points are set as 40%, 80%, and 10% (postpeak) of the peak strength, respectively.

The first point displacement is determined based on the force level and the initial stiffness of the test curve, and the second point displacement is used for adjusting the linear backbone model's energy dissipation (area bounded by the abscissa and multisegment linear backbone) to be the same as the idealized backbone before the peak strength. Similarly, the fourth point displacement is utilized to balance the energy dissipation after the peak strength. For the monotonic test curves, the test curve itself is an idealized backbone, and the same multisegment linear backbone phenomenological model is adopted.

Additionally, in some test data characterization results, the measured first point displacement value (at 40% P_u) is quite, small implying that the connection might undergo precompression before testing. The deformation is bounded based on an estimate of the first linear segment stiffness P_1/D_1 as described in the test report (Zhang and Schafer 2020). Further, some tests demonstrate two peak strengths, where the displacement magnitude at the first peak is quite small (essentially linear response), and the second peak strength is only a few percent lower than the first peak but occurs at larger deformation and is observed to have bearing damage. In these cases, for the backbone fitting the force of the third point in the backbone model is set as the actual peak strength, but the displacement is set as the same as the second peak. Overall, this linear backbone phenomenological model can capture the initial stiffness, peak strength and displacement, and postpeak behavior, as well as the energy dissipation of the experimental data. Additional data characterization to provide the unloading, reloading,

Fig. 10. Deformation and failure of a 97-12-30 test with thin sheet buckling toward the fastener head: (a) peak strength level front view; (b) peak strength level side view; (c) 80% postpeak strength level; and (d) after test.

pinching, and energy-degradation parameters for a complete Pinching 4 material model remain for future work.

Individual, fitted, multisegment linear backbone results for each test are provided in the test report (Zhang and Schafer 2020). It is expected for modeling in steel sheet shear walls that average backbone curves of the connections will be used; therefore, averaged results, even with all their simplifications, are provided here. For the test series with sensitivity to buckling direction, the averaging is the most approximate, as illustrated for the 54-8-30 test series in Fig. 15, where averages of the monotonic tests and cyclic tests (including depending on direction of buckling for the thin sheet) are all provided. The average cyclic response is recommended for modeling connections in steel sheet shear walls, as summarized in Table 6.

Specifically, these response models can be used to improve the effective strip method (Yanagi and Yu 2014) in AISI S400 (AISI 2015), particularly for predicting the nonlinear pushover deformation of steel sheet shear walls. In addition, these response models can be used directly in a more sophisticated shear wall simulation, similar to that employed by Buonopane et al. (2015), to predict the strength of steel sheet shear walls with unique detailing or configurations. Preliminary work in this regard demonstrated that accurate modeling of the connection is crucial to overall prediction of the shear wall strength and deformation capacity.

Ductility Evaluation

Recent work on the in-plane shear performance of steel deck diaphragm systems (Torabian and Schafer 2021; Schafer 2019) has shown that the deformation-based ductility of screw-fastened connections is integral to the ductility of the larger system. Connection ductility has now been embedded directly in performance requirements for steel deck diaphragms in AISI S400 (AISI 2020). It is possible that similar ductility requirements may be sought for steel sheet shear wall connections because the in-plane performance of the shear wall is similar to a diaphragm. To that end, two ductility indices $\mu_1 = D_{80\%}/D_y$ and $\mu_2 = D_u/D_y$ are introduced herein to assess the ductility of different connection configurations. As provided in Fig. 16(a), D_y is the displacement level calculated with the peak force and initial stiffness, and $D_{80\%}$ and D_u refer to the displacement level corresponding to the 80% and 10% postpeak force levels.

The average ductility index values of the cyclic tests for each test series are tabulated in Table 7. The test ductility index mean value and standard deviation are presented in Fig. 16(b). The index μ_1 is more consistent than index μ_2 because D_u relies on the test ending deformation, where D_u can be quite large if a complete disengagement develops. All the connection configurations in this test program demonstrate reasonably high levels of ductility, with the averaged index μ_1 having a minimum of 25 and an average of 50.

Focusing on μ_1 to discuss the results, when the only change in the configuration is the fastener size, larger #10 fasteners typically result in lower ductility than #8 fasteners (average μ_1 decreased from 56 down to 42), although there are individual exceptions as in the case of the 54-(8 or 10)-30 series.

The 2.46-mm (97-mil) framing ply test series commonly features higher ductility ($\mu_1 = 59$ on average) than the 1.37-mm

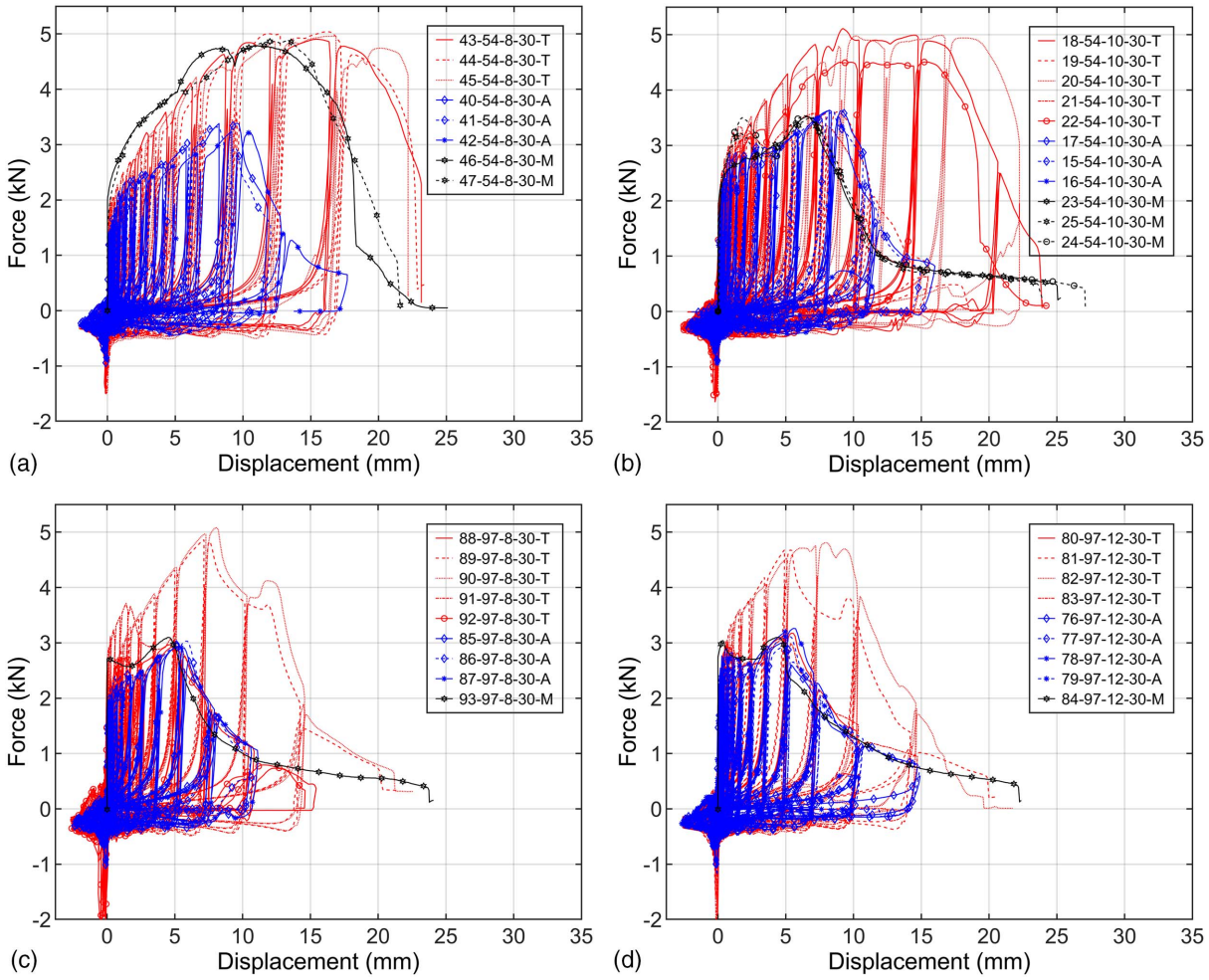

Fig. 11. Force-displacement curves of four test series with similar sheet and framing thickness: (a) 54-8-30; (b) 54-10-30; (c) 97-8-30; and (d) 97-12-30.

(54-mil) framing ply test series ($\mu_1 = 43$ on average) under the same conditions. Presumably, this is because the 2.46-mm (97-mil) framing ply is relatively thicker than the thin steel sheet ply, resulting in constraining the fastener tilting, and more energy can be dissipated through the thin steel sheet ply deformation in pure bearing and shear rupture. Additionally, no clear relationship between thin steel sheet ply thickness and connection ductility is observed.

Code Strength Predictions

The failure modes observed in this testing program include bearing, tilting and bearing, pull-through, and shear rupture. The bearing or tilting and bearing strength limit states develop before the pull-through or shear rupture. The connection test strength can be predicted by the screw shear strength limited by tilting and bearing provisions in J4.3.1 in the AISI S100 (AISI 2016), as shown in Eqs. (1)–(3)

$$P_{nv} = 4.2(t_2^3 d)^{1/2} F_{u2} \tag{1}$$

$$P_{nv} = 2.7 t_1 d F_{u1} \tag{2}$$

$$P_{nv} = 2.7 t_2 d F_{u2} \tag{3}$$

where t_1 and F_{u1} = thickness and ultimate strength of the steel sheet in contact with the screw head (always the thinner sheet ply in the tests here); t_2 and F_{u2} = thickness and ultimate strength of the steel sheet not in contact with the screw head (the framing ply in the tests here); and d = screw diameter. For $t_2/t_1 \leq 1.0$, nominal screw shear strength limited by tilting, and bearing P_{nv} shall be taken as the smallest value of Eqs. (1)–(3). Per AISI S100 for $t_2/t_1 \geq 2.5$, P_{nv} shall be taken as the smaller of Eqs. (2) and (3). Interpolation is needed if $2.5 > t_2/t_1 > 1.0$. In the specimens studied here, t_2/t_1 is always larger than 2.5 except for the 54-(8 or 10)-30 series, and the shear strength for the connections tested herein are limited by the thin steel sheet bearing, which can be predicted with Eq. (2). Comparison of the test to code strength is provided as ratios in Fig. 17(a).

Shear rupture is commonly observed in the tests at final failure. For comparison purposes, we also evaluated the connection strength limited by shear rupture based on the bolted connection provision from J6.1-1 in AISI S100 (AISI 2016), as presented in Eq. (4)

$$P_{\text{net}} = 0.6 F_{u1} 2 t_1 e_{\text{net}} \tag{4}$$

where e_{net} = clear distance between end of material and edge of fastener hole; and P_{net} = connection shear strength limited by shear rupture. The test and prediction strength values are normalized with

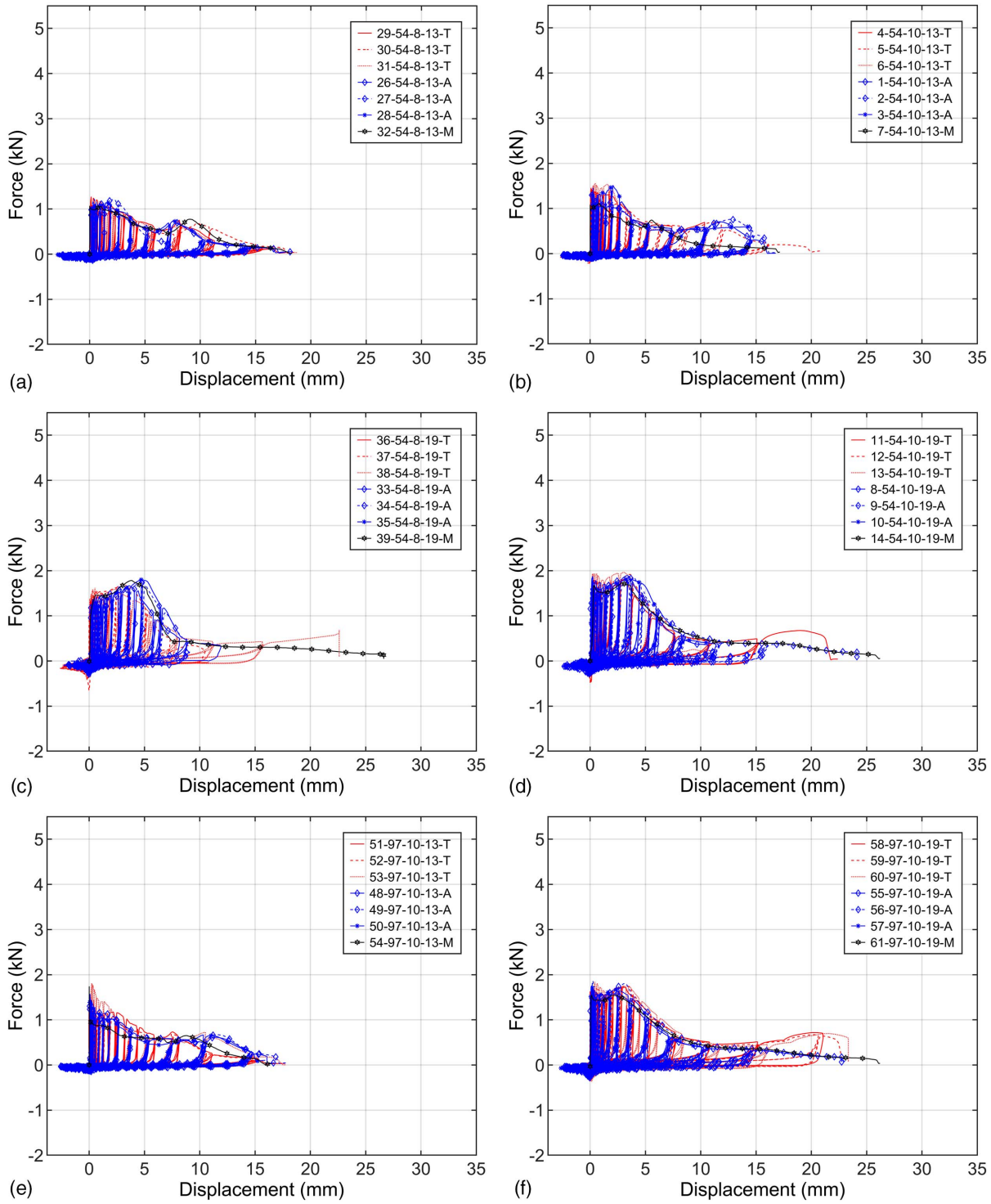

Fig. 12. Force-displacement curves of six test series with sheet and framing thickness far apart: (a) 54-8-13; (b) 54-10-13; (c) 54-8-19; (d) 54-10-19; (e) 97-10-13; and (f) 97-10-19.

$t_1 F_{u1} w$, where w implies the specimen width taken as 50.8-mm (2-in.) herein, as shown in Fig. 17(b).

As presented in Fig. 17(a), tests with the thin 0.33-mm (13-mil) and 0.48-mm (19-mil) steel sheet ply demonstrate test-to-predicted ratios lower than 1, i.e., unconservative predictions. It can further be observed from Fig. 17(a) that when the sheet plies are in the same configuration the test-to-predicted ratio typically decreases with the increase of the screw diameter. By normalizing to the ideal strength $t_1 F_{u1} w$, as given in Fig. 17(b), one can observe that the cases with 0.76-mm (30-mil) sheet ply, in which the buckling of the thin sheet ply is toward the fastener head, have strength consistent with shear rupture. In contrast, all other tests, including the same configurations but with buckling of the thin ply in the opposite direction, have strength closer to the bearing capacity. The AISI S100 screw-fastened connection provisions, calibrated to experiments by Peköz (1990), were never intended for application to steel sheets less than 0.724-mm (28-mil), and thus modifications are needed to extend the provisions to these ranges.

To correct the unconservative shear strength predictions for the test series with 0.33-mm (13-mil) and 0.48-mm (19-mil) steel sheet

plies, the tilting and bearing provisions, specifically Eq. (2), are revisited. Development of this expression did not consider such a thin sheet, where piling of material in front of the screw head is as common as tearing. A simple linear reduction is proposed, where

$$P_{nv} = 2.7R_t t d F_u \tag{5}$$

$$R_t = 1 \quad \text{if } t \geq 0.79 \text{ mm (31 mil or 0.031 in.)} \tag{6}$$

$$R_t = 13.37t/\alpha + 0.59 \quad \text{if } t < 0.79 \text{ mm (31 mil or 0.031 in.)} \tag{7}$$

$$\alpha = 25.4 \quad \text{if } t \text{ is in millimeters} \tag{8a}$$

$$\alpha = 1 \quad \text{if } t \text{ is in inches} \tag{8b}$$

The linear fit is selected based on the mean test-to-code predicted strength ratio of 54-8-13, 97-10-19, and 97-12-30 test series, whose strength ratio are the lowest among the test series with a 0.33-mm (13-mil), 0.48-mm (19-mil), and 0.76-mm (30-mil) thin steel sheet, respectively, depicted as circles in Fig. 18(a). The linear reduction R_t is thus proposed for steel sheet screw-fastened connections of standard CFS framed steel sheet sheathed shear walls with sheathing thickness less than 0.79-mm (31-mil), as presented in Eqs. (5)–(8).

The adjusted code strength prediction value P^*_{nv} are utilized for test-to-predicted ratio calculation and provided in Fig. 18(b). The average and coefficient of variation (COV) of the test-to-predicted ratio for all cyclic tests in the test series with 0.33-mm (13-mil) and 0.48-mm (19-mil) are improved from 0.86 and 0.10 without the R_t correction to 1.07 and 0.11 with the correction. If only the monotonic data are considered, which would be common in developing connection strength expressions for AISI S100, the average and COV improve from 0.83 and 0.18 to 1.04 and 0.19 for the considered data.

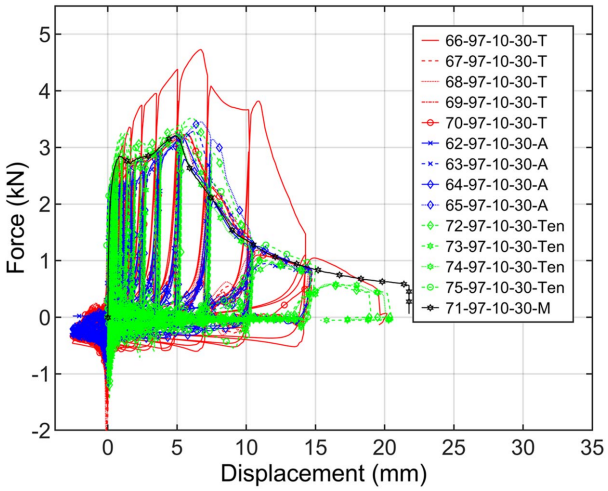

Fig. 13. Force-displacement curve of test series 97-10-30.

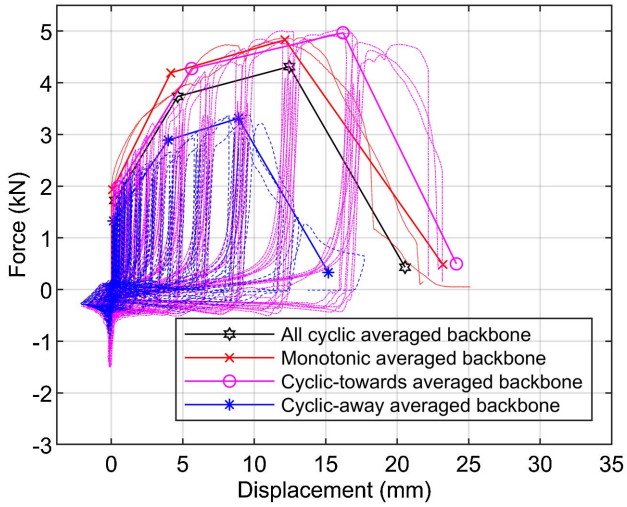

Fig. 15. Test data characterization average values for the 54-8-30 test series.

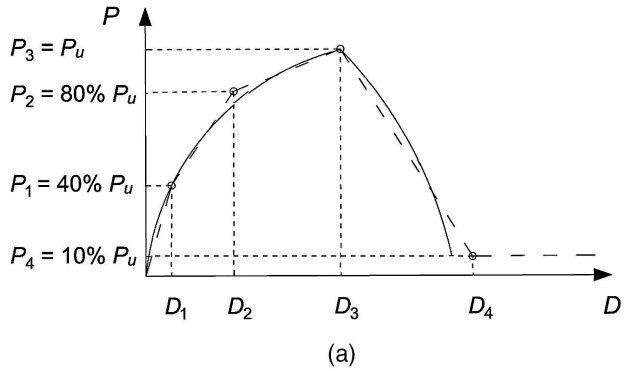

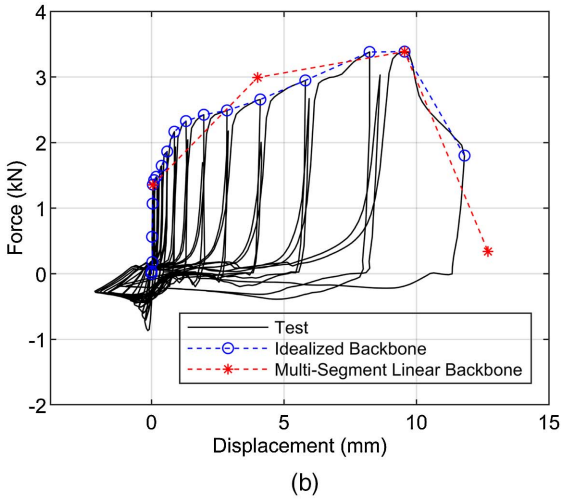

Fig. 14. Backbone data characterization based on equivalent cumulative energy dissipation: (a) test data characterization diagram; and (b) characterization of a test in the 54-8-30 test series.

Table 6. Average four-point backbone values for cyclic tests

Test series	D_1 (mm)	D_2 (mm)	D_3 (mm)	D_4 (mm)	P_1 (kN)	P_2 (kN)	P_3 (kN)	P_4 (kN)
54-8-13	0.06	0.11	1.04	13.13	0.45	0.97	1.14	0.11
54-10-13	0.08	0.13	1.07	13.65	0.54	1.13	1.34	0.13
97-10-13	0.04	0.07	0.10	12.11	0.60	1.20	1.51	0.15
54-8-19	0.07	0.53	3.39	11.50	0.67	1.44	1.67	0.17
54-10-19	0.07	0.13	3.36	11.53	0.75	1.57	1.88	0.19
97-10-19	0.05	0.10	2.88	14.61	0.70	1.47	1.75	0.18
54-8-30	0.31	4.80	12.55	19.66	1.66	3.58	4.14	0.41
54-10-30	0.14	2.98	10.23	18.85	1.63	3.52	4.08	0.41
97-8-30	0.07	1.58	5.32	13.68	1.42	3.01	3.56	0.36
97-10-30	0.08	1.66	5.70	13.88	1.36	2.93	3.41	0.34
97-12-30	0.05	0.75	5.45	14.02	1.40	2.88	3.51	0.35

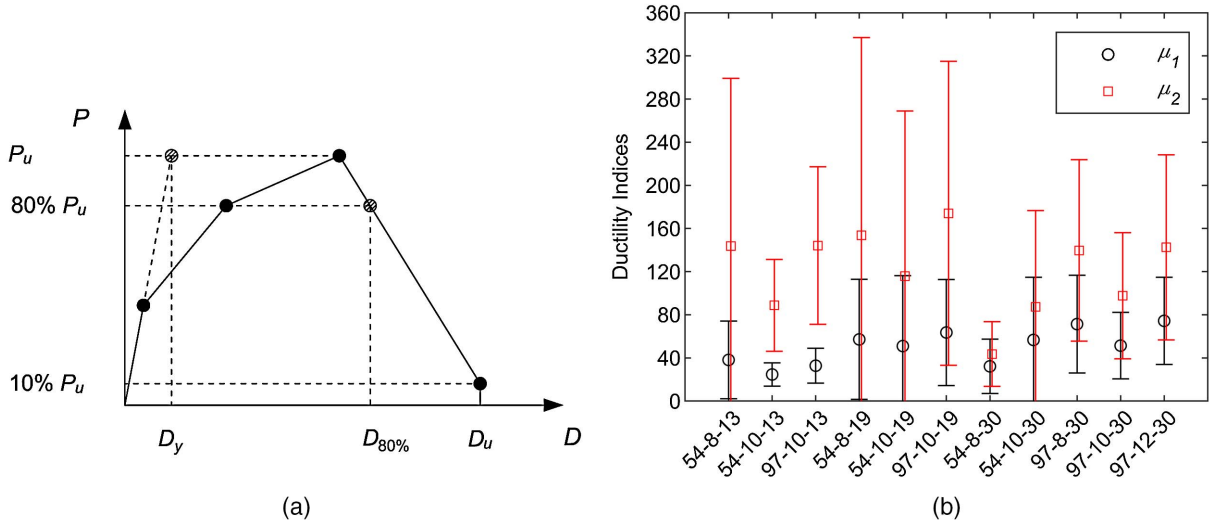

Fig. 16. Test ductility index: (a) test displacement level diagram; and (b) test ductility indices.

Table 7. Average ductility indices for cyclic tests

Test series	D_y (mm)	$D_{80\%}$ (mm)	D_u (mm)	μ_1	μ_2
54-8-13	0.14	3.73	13.13	38.15	143.72
54-10-13	0.20	3.87	13.65	24.65	88.74
97-10-13	0.10	2.77	12.11	32.78	144.18
54-8-19	0.17	5.19	11.50	57.17	153.75
54-10-19	0.19	5.18	11.53	50.99	115.95
97-10-19	0.14	5.49	14.61	63.58	174.04
54-8-30	0.78	14.13	19.66	32.21	43.57
54-10-30	0.35	12.14	18.85	56.69	87.38
97-8-30	0.16	7.18	13.68	71.36	139.68
97-10-30	0.20	7.52	13.88	51.39	97.63
97-12-30	0.13	7.36	14.02	74.37	142.57

Summary and Conclusions

The seismic performance of CFS framed screw-fastened steel sheet sheathed shear walls is significantly influenced by the nonlinear cyclic response of the connection between the framing and steel sheet sheathing. Further, the impact of the steel sheet shear buckling on the strength and ductility of this critical connection should be considered. Little data exist for the behavior of these connections in shear, especially cyclic data at the relevant combinations of thin steel sheet and thick steel framing. A cyclic lap shear testing protocol is developed with small compression displacements to buckle the thin sheet ply. The setup is found to be appropriate for investigating the impact of sheet buckling and the resulting shear–tension interaction demand on the connection response.

For configurations where the framing and sheet thickness are relatively close [e.g., 1.37-mm (54-mil) framing and 0.76-mm (30-mil) sheet], the test strength is sensitive to the direction in which the thin steel sheet ply is buckled. When the sheet ply buckles away from the fastener head, it can create additional tension demand on the connection, which can trigger a pull-through limit state that degrades the strength and postpeak shear behavior of the connection. For configurations where the framing and sheet thickness are far apart [e.g., 1.37-mm (54-mil) or 2.46-mm (97-mil) framing with 0.33-mm (13-mil) or 0.48-mm (19-mil) sheet], the test strength is not sensitive to the buckling direction of the thin steel sheet ply. Nonetheless, the buckling of the thin ply still influences the results because the additional shear–tension interaction demand on the connection degrades the strength modestly and influences the postpeak response.

All screw-fastened connection configurations exhibit good ductility in this test program. In most cases, larger size screws, e.g., #10 versus #8, demonstrate lower ductility, whereas thicker 2.46-mm (97-mil) framing has higher ductility than 1.37-mm (54-mil) framing. Screw shear strength limited by the tilting and bearing provision in J4.3.1 of AISI S100 (AISI 2016) provides

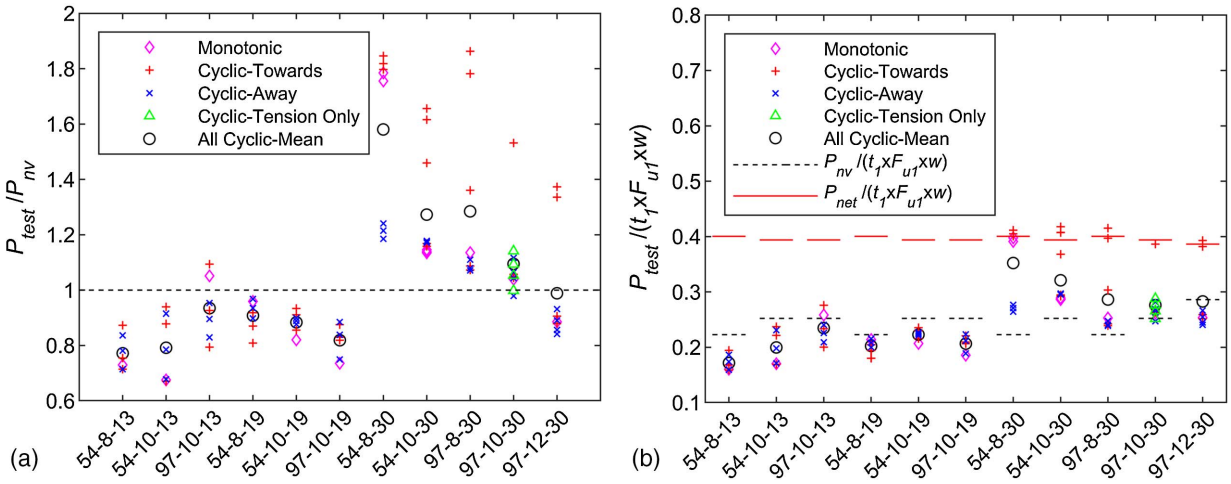

Fig. 17. Test strength and code strength predictions: (a) test-to-code predicted strength ratio; and (b) normalized test strength and code strength predictions.

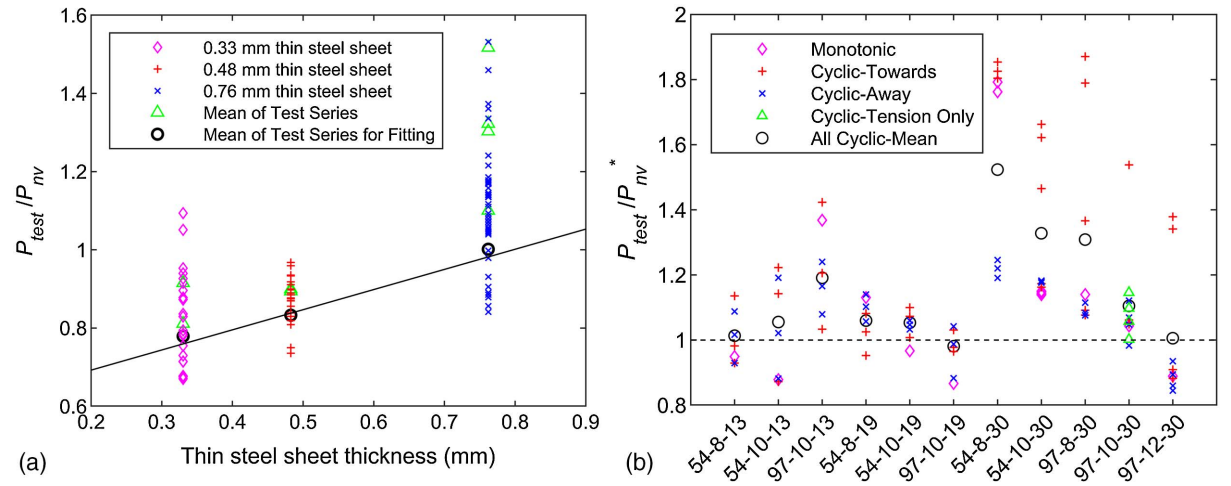

Fig. 18. Code-predicted strength adjustment: (a) linear fitting for test-to-code-predicted strength ratio; and (b) test-to-code-predicted strength ratio after adjustment.

reasonable shear strength predictions for connections with the 0.76-mm (30-mil) sheet, but an adjustment is required for thinner 0.33-mm (13-mil) or 0.48-mm (19-mil) steel sheets. The cyclic screw-fastened connection testing data and the multilinear backbone curve generated by characterization of the testing provide critical missing information for the design and simulation of cold-formed steel framed steel sheet sheathed shear walls.

Data Availability Statement

Some or all data, models, or code that support the findings of this study are available from the corresponding author upon reasonable request.

Acknowledgments

This work is part of the research project Seismic Resiliency of Repetitively Framed Mid-Rise Cold-Formed Steel Building (CFS-NHERI), which is supported by the National Science Foundation under Grant Nos. 1663348 and 1663569. Test materials provided by ClarkDietrich are gratefully acknowledged. The tests conducted herein were assisted by Gbenga Olaolorun, Joel John, Boyu Qian, and Nick Logvinovsky; the authors would like to express gratitude to their great help.

Disclaimer

Any opinions, findings, and conclusions or recommendations expressed in this publication are those of the authors and do not necessarily reflect the views of the sponsors and employers.

References

AISI (American Iron and Steel Institute). 2013. *Test standard for cold-formed steel connections*. AISI S905-13. Washington, DC: AISI.

AISI (American Iron and Steel Institute). 2015. *North American standard for seismic design of cold-formed steel structural systems*. AISI S400-15. Washington, DC: AISI.

AISI (American Iron and Steel Institute). 2016. *North American specification for the design of cold-formed steel structural members*. AISI S100-16. Washington, DC: AISI.

AISI (American Iron and Steel Institute). 2020. *North American standard for seismic design of cold-formed steel structural systems*. AISI S400-20. Washington, DC: AISI.

ASTM. 2016. *Test methods for tension testing of metallic materials*. ASTM E8/E8M. West Conshohocken, PA: ASTM.

Brière, V., and C. A. Rogers. 2017. *Higher capacity cold-formed steel sheathed and framed shear walls for mid-rise buildings: Part 2*. Research Rep. No. RP17-6. Montréal: Dept. of Civil Engineering and Applied Mechanics, McGill Univ.

Buonopane, S. G., G. Bian, T. H. Tun, and B. W. Schafer. 2015. "Computationally efficient fastener-based models of cold-formed steel shear walls with wood sheathing." *J. Constr. Steel Res.* 110: 137–148. https://doi.org/10.1016/j.jcsr.2015.03.008.

DaBreo, J., N. Balh, C. Ong-Tone, and C. A. Rogers. 2014. "Steel sheathed cold-formed steel framed shear walls subjected to lateral and gravity loading." *Thin-Walled Struct.* 74 (1): 232–245. https://doi.org/10.1016/j.tws.2013.10.006.

FEMA. 2007. *Interim testing protocols for determining the seismic performance characteristics of structural and nonstructural components*. FEMA 461. Washington, DC: FEMA.

Madsen, R. L., T. A. Castle, and B. W. Schafer. 2016. *Seismic design of cold-formed steel lateral load-resisting systems*. NEHRP Seismic Design Technical Brief No. 12. Gaithersburg, MD: NIST.

Mazzoni, S., F. McKenna, M. H. Scott, and G. L. Fenves. 2006. *OpenSees command language manual*. Berkeley, CA: Pacific Earthquake Engineering Research Center.

Morgan, K. A., M. A. Sorhouet, and R. L. Serrette. 2002. *Performance of CFS framed shear walls—Alternative configurations*. Rep. No. LGSRG-06-02. Santa Clara, CA: Santa Clara Univ.

Ong-Tone, C., and C. A. Rogers. 2009. *Tests and evaluation of cold-formed steel frame/steel sheathed shear walls*. Research Rep. Montréal: Dept. of Civil Engineering and Applied Mechanics, McGill Univ.

Peköz, T. 1990. "Design of cold-formed steel screw connections." In *Proc., 10th Int. Specialty Conf. on Cold-Formed Steel Structures*, 575–587. St. Louis: Univ. of Missouri.

Peterman, K. D., N. Nakata, and B. W. Schafer. 2014. "Hysteretic characterization of cold-formed steel stud-to-sheathing connections." *J. Constr. Steel Res.* 101 (Oct): 254–264. https://doi.org/10.1016/j.jcsr.2014.05.019.

Rizk, R., and C. A. Rogers. 2017. *Higher strength cold-formed steel framed/steel shear walls for mid-rise construction*. Research Rep. Montréal: Dept. of Civil Engineering and Applied Mechanics, McGill Univ.

Rogers, C. A., N. Balh, C. Ong-Tone, I. Shamim, and J. DaBreo. 2011. "Development of seismic design provisions for steel sheet sheathed shear walls." In *Proc., Structures Congress 2011*, 676–687. Reston, VA: ASCE.

Rogers, C. A., and R. Tremblay. 2003. "Inelastic seismic response of side lap fasteners for steel roof deck diaphragms." *J. Struct. Eng.* 129 (12): 1637–1646. https://doi.org/10.1061/(ASCE)0733-9445(2003)129:12(1637).

Santos, V., and C. A. Rogers. 2017. *Higher capacity cold-formed steel sheathed and framed shear walls for mid-rise buildings: Part 1*. Research Rep. Montréal: Dept. of Civil Engineering and Applied Mechanics, McGill Univ.

Schafer, B. W. 2019. "Research on the seismic performance of rigid wall flexible diaphragm buildings with bare steel deck diaphragms." CFSRC Rep. Accessed January 27, 2019. http://jhir.library.jhu.edu/handle/1774.2/60360.

Serrette, R. L., J. Encalada, B. Matchen, H. Nguyen, and A. Williams. 1997. *Additional shear wall values for lightweight steel framing*. Rep. No. LGSRG-1-97. Santa Clara, CA: Santa Clara Univ.

Shamim, I., J. DaBreo, and C. A. Rogers. 2013. "Dynamic testing of single- and double-story steel sheathed cold-formed steel-framed shear walls." *J. Struct. Eng.* 139 (5): 807–817. https://doi.org/10.1061/(ASCE)ST.1943-541X.0000594.

Shi, Y., S. Torabian, B. W. Schafer, W. S. Easterling, and M. R. Eatherton. 2018. "Sidelap and structural fastener tests for steel deck diaphragms." In *Proc., Wei-Wen Yu Int. Specialty Conf.: Cold-Formed Steel Structures*. Rolla, MO: Wei Wen Yu Center for Cold-Formed Steel Structures.

Singh, A., X. Wang, and T. C. Hutchinson. 2021. *Lateral response of cold-formed steel framed steel sheathed in-line wall systems detailed for mid-rise buildings. Part I: Shake table test phase*. Structural Systems Research Project Rep. No. SSRP-19/05. La Jolla, CA: Univ. of California, San Diego.

Tao, F., A. Chatterjee, and C. D. Moen. 2016. *Monotonic and cyclic response of single shear cold-formed steel-to-steel and sheathing-to-steel connections*. Rep. No. CE/VPI-ST-16/01. Blacksburg, VA: Virginia Tech.

Torabian, S., and B. W. Schafer. 2021. "Cyclic experiments on sidelap and structural connectors in steel deck diaphragms." *J. Struct. Eng.* 147 (4): 04021028. https://doi.org/10.1061/(ASCE)ST.1943-541X.0002981.

Yanagi, N., and C. Yu. 2014. "Effective strip method for the design of cold-formed steel framed shear wall with steel sheet sheathing." *J. Struct. Eng.* 140 (4): 04013101. https://doi.org/10.1061/(ASCE)ST.1943-541X.0000870.

Yu, C., and Y. Chen. 2009. *Steel sheet sheathing options for cold-formed steel framed shear wall assemblies providing shear resistance—Phase 2*. Rep. No. UNT-G70752. Denton, TX: Dept. of Engineering Technology, Univ. of North Texas.

Yu, C., H. Vora, T. Dainard, J. Tucker, and P. Veetvkuri. 2007. *Steel sheet sheathing options for cold-formed steel framed shear wall assemblies providing shear resistance*. Rep. No. UNT-G76234. Denton, TX: Dept. of Engineering Technology, Univ. of North Texas.

Zhang, Z., and B. W. Schafer. 2019. "Simulation of steel sheet sheathed cold-formed steel framed shear walls." In *Proc., Annual Stability Conf.-Structural Stability Research Council*. St. Louis: Structural Stability Research Council, American Institute of Steel Construction.

Zhang, Z., and B. W. Schafer. 2020. "Test report: Cyclic performance of steel sheet connections for CFS steel sheet shear walls." CFSRC Rep. No. R-2020-06. Accessed July 30, 2020. http://jhir.library.jhu.edu/handle/1774.2/62850.